Additively manufactured respirators: quantifying particle transmission and identifying system-level challenges for improving filtration efficiency

Lindsey B. Bezek [a], Jin Pan [b], Charbel Harb [b], Callie E. Zawaski [a], Bemnet Molla [a], Joseph R. Kubalak [a], Linsey C. Marr [b], Christopher B. Williams [a],*

[a] Department of Mechanical Engineering, Virginia Tech, Blacksburg, VA, 24061, United States
[b] Department of Civil and Environmental Engineering, Virginia Tech, Blacksburg, VA, 24061, United States

ARTICLE INFO

ABSTRACT

The COVID-19 pandemic has disrupted the supply chain for personal protective equipment (PPE) for medical professionals, including N95-type respiratory protective masks. To address this shortage, many have looked to the agility and accessibility of additive manufacturing (AM) systems to provide a democratized, decentralized solution to producing respirators with equivalent protection for last-resort measures. However, there are concerns about the viability and safety in deploying this localized download, print, and wear strategy due to a lack of commensurate quality assurance processes. Many open-source respirator designs for AM indicate that they do not provide N95-equivalent protection (filtering 95% of SARS-CoV-2 particles) because they have either not passed aerosol generation tests or not been tested. Few studies have quantified particle transmission through respirator designs outside of the filter medium. This is concerning because several polymer-based AM processes produce porous parts, and inherent process variation between printers and materials also threaten the integrity of tolerances and seals within the printed respirator assembly. No study has isolated these failure mechanisms specifically for respirators. The goal of this paper is to measure particle transmission through printed respirators of different designs, materials, and AM processes. The authors compare the performance of printed respirators to N95 respirators and cloth masks. Respirators in this study printed using desktop- and industrial-scale fused filament fabrication processes and industrial-scale powder bed fusion processes were not sufficiently reliable for widespread distribution and local production of N95-type respiratory protection. Even while assuming a perfect seal between the respirator and the user's face, although a few respirators provided >90% efficiency at the 100−300 nm particle range, almost all printed respirators provided <60% filtration efficiency. Post-processing procedures including cleaning, sealing surfaces, and reinforcing the filter cap seal generally improved performance, but the printed respirators showed similar performance to various cloth masks. The authors further explore the process-driven aspects leading to low filtration efficiency. Although the design/printer/material combination dictates the AM respirator performance, the identified failure modes originate from system-level constraints and are therefore generalizable across multiple AM processes. Quantifying the limitations of AM in producing N95-type respiratory protective masks advances understanding of AM systems toward the development of better part and machine designs to meet the needs of reliable, functional, end-use parts.

1. Introduction

The novel coronavirus disease (COVID-19) pandemic has highlighted urgent supply chain and manufacturing concerns with respect to personal protective equipment (PPE) for medical professionals and first responders. In particular, N95-type respiratory protective masks are needed to address the spread of airborne severe acute respiratory syndrome coronavirus 2 (SARS-CoV-2) particles. Typical N95 respirators both reduce droplet transmission and provide breathability through their use of non-woven nanofibers that retain static charge, and they are capable of filtering 95% of particles at the size of 300 nm. The filtration efficiency, proper fit, and user comfort of N95 respirators are critical requirements that increase manufacturing complexity, cost, and delays. N95 respirators are manufactured on a global scale, and a substantial

portion of the supply in the United States is manufactured overseas. The complexity and scale of this supply chain create additional challenges to scaling manufacturing in emergent circumstances.

In response to this shortage, efforts have launched at the governmental, industrial, academic, and even individual level to fabricate PPE such as respirators and masks [1]. Respirators are designed to filter airborne particles. They are meant to be properly fitted and have clearly marked levels of approval (e.g., N95). Some particulate respirators are approved by the United States Food and Drug Administration (FDA) for use as surgical respirators. Masks, on the other hand, are not meant to filter airborne particles and are loosely fitted. Some masks are approved by the FDA for use as surgical masks, which are not meant to provide respiratory protection [2]. For protection against SARS-CoV-2 particles, N95 respirators are superior to surgical masks and cloth varieties, but their shortage has prompted the United States Centers for Disease Control and Prevention (CDC) to relax PPE recommendations for healthcare personnel [2,3].

Additive manufacturing (AM), also commonly known as 3D printing, could provide an avenue for scaled-up production of respirators for healthcare workers. The AM industry is capable of providing a wide variety of customized part designs to address the spread of COVID-19, helping to alleviate the strain on established supply chains struggling to keep up with the demand for PPE [4,5]. It is therefore of interest to determine the filtration capabilities of available designs of respirators (commonly referred to as "3D printed face masks") to determine if the respirators could meet the N95 threshold criteria and see how they compare to cloth masks.

1.1. Additive manufacturing considerations

Many have looked to AM to rapidly generate respirators for use only if the N95 supply were depleted [6–9]. AM processes offer flexibility and agility to fabricate complex respirator shapes without additional tooling or changeover time. AM has previously been successful at distributed manufacturing strategies [10]. Companies with AM systems, regardless of their industry, could shift to fabricating PPE without the need to modify factory layouts or manufacturing equipment. A multitude of industrial systems could be utilized worldwide [5], and hobbyists with desktop-scale 3D printers could also get involved, as digital designs can be rapidly disseminated for local production of PPE.

The fused filament fabrication (FFF) AM process, which operates by selectively extruding thermoplastic materials, is the most accessible technology in terms of both required skill to operate and number of printers in the market. For desktop-scale FFF systems, the two most common materials are acrylonitrile butadiene styrene (ABS) and polylactic acid (PLA). Industrial-scale FFF systems are capable of printing with engineering-grade thermoplastics (e.g., ULTEM), which could be advantageous for producing reusable respirators that can survive the temperatures and pressures of autoclave sterilization. Polymer powder bed fusion (PBF) processes (including polymer laser sintering and Multi-Jet Fusion), which use infrared radiation energy to melt and coalesce polymer powder, have been investigated as the commonly-used nylon-12 material is also autoclavable for sterilization. Additionally, the use of a polymer powder bed inherently provides support and thus enables printing numerous respirators throughout the entire print volume to appreciably scale production.

While efforts are ongoing to use AM to fabricate PPE, such as respirators, as an emergency back-up supply, the protection offered by such PPE is unknown and likely inferior to medical-grade equipment without ample time for rigorous testing and inspection [11]. One concern about the efficacy of using AM to produce respirators is the intrinsic porosity in FFF- and PBF-produced parts, which can affect filtration efficiency, accuracy, and reliability of the printed respirators. In FFF processes, porosity can result from adjacent layers not fully fusing [12,13], gaps left from changing direction and stopping/starting melt extrusion, and/or gaps left from adjacent extruded paths failing to fuse together

[14,15]. Such inherent, process-induced defects have been shown to cause up to 32% porosity in FFF parts, with 200–800 μm diameter pores [16], which could render them ineffective in protecting against 0.3 μm virus particles. In addition, this porosity from layer-wise fabrication [16] reduces strength and stiffness [13,15] and is detrimental for parts designed for contact with gases [14], as is the case with respirators. Similarly, parts produced via PBF can be up to 30% porous [17] due to insufficient delivery of energy, recoating defects, and/or the use of heavily recycled powder.

One solution to mitigate porosity in printed polymer parts is to seal them in a post-processing step. For example, an aqueous acetone solution has been successfully applied to printed ABS material for sealing microfluidic channels [18], but chemical polishing can erode geometric features [19]. Post-process heating has potential to further coalesce the printed polymer to eliminate porosity, but at the expense of dimensional instability [20]. These post-process techniques can be labor-intensive and have not been evaluated for their ability to affect nanoparticle transmission. This lack of research also prevents their adoption into standardized operating procedures to guide their manual deployment.

Another anticipated challenge in the use of AM to directly fabricate PPE through shared digital designs is the inherent variability between AM machines, materials, and build parameters [21], which can affect the mechanical properties of the printed materials and the accuracy of the printed geometries. In FFF, processing parameters such as layer thickness [12], layer orientation [22], raster width and spacing [23], and filament feed rate [14] influence porosity, part quality, and performance. Prior round robin studies have shown variation between parts/tolerances despite parts being made on similar FFF systems [24–26]. Due to these inherent machine-to-machine differences, although FFF systems' toolpaths can be modified [14], and product design parameters [27] or process parameters [19] can be fine-tuned to account for anticipated shortcomings, it is uncertain whether these parameters can be readily transferred between different systems of the same type to produce identical parts. In addition, FFF printers are prone to misfeed defects, which, if undetected, pose a challenge for scaling up production if the respirators cannot be adequately qualified. Quality of filament (e.g., inconsistent diameter, moisture uptake) can also affect the resultant mechanical properties [28]. Similar to FFF, the PBF process exhibits variation between different machines, materials, and process parameters (including layer thickness, laser power, hatch spacing, and bed temperature). Variations in PBF process parameters affect energy density delivered to the powder bed, which result in microscale porosity [29] and cause variation in mechanical properties [30]. Powder quality (whether virgin powder or recycled) also affects porosity [31]. The FDA has issued further technical guidelines for medical devices fabricated with AM that supplement the aforementioned considerations [32].

1.2. Printed respirator design principles and potential failure modes

While many different printable respirator designs have surfaced, all follow a similar overall design to satisfy the key functional needs of (i) meeting a standard of filtering (e.g., 95% of particles sized 300−500 nm), (ii) providing a good fit and seal against the user's face with a straightforward means of securing, (iii) being lightweight, and (iv) being easy to clean (e.g., minimal crevices, smooth contours) if meant to reuse. Most designs are composed of an assembly of multiple printed pieces (Fig. 1). The shell provides the main body and fits against the user's face. A separate filter cap is press-fit against the shell to secure the filter medium. The filter medium must achieve adequate airborne particle filtration while permitting breathability (i.e., low pressure drop) and ease of filter replacement. Interfaces between each of the components must be properly sealed to ensure all airflow to the user passes through the filter medium.

In review of several available, printable respirator designs, the authors identify four potential modes of failure in which printed respirators could provide a user with lower than expected filtration efficiency.
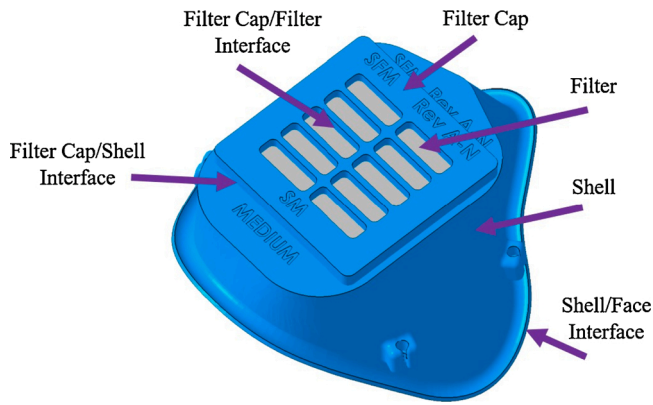
Fig. 1. Schematic of the Stopgap Surgical Face Mask [33] with terminology and potential modes of failure identified.

Fig. 1 identifies these modes on the Stopgap Surgical Face Mask [33] as an example.

- *Shell porosity.* Penetration through the printed shell could significantly reduce filtration efficiency. Geometric design constraints (including respirator shape and thickness) and print orientation have not been universally established; these design and processing decisions directly affect the resultant porosity of FFF parts due to defects from tool-pathing, interlayer adhesion, and support structures [14].
- *Shell/Face interface.* A common and critical failure mode in traditional N95 respirators is a poor fit to the user's face. A good fit is paramount because if the respirator does not conform to the contours of the face, particles could be inhaled [34]. As such, the United States National Institute for Occupational Safety and Health (NIOSH) requires qualitative fit testing for users before new respirator models are used [35]. Shells printed from rigid polymers might not adequately conform to a user's face to provide a proper seal. Many distributed designs attempt to compensate for this by offering several scaled versions of the design in an effort to offer different sizes for users (e.g., Small/Medium/Large). Unlike traditional manufacturing methods, AM provides an opportunity to mass-customize individually fitting respirators [6]; however, this would require acquisition and conversion of 3D scan data of every user, which could significantly impede production throughput.
- *Filter Cap/Shell interface.* In many designs, the filter medium is secured with a separately printed filter cap that is press-fit onto the shell. Depending on the designed (and resultant printed) tolerances of this interface, particles could flow between the cap and the shell and bypass the filter medium.
- *Filter Cap/Filter interface.* Although the filter medium would be selected based on its ability to block a certain threshold of particles of a certain size (e.g., 95%, 99%), the filtration efficiency of the respirator will be insufficient if the filter does not adequately cover the exposed area. Similarly, if the filter is not rigidly secured within the filter cap assembly, particles may be able to flow around the medium.

Due to these identified failure modes, which result from both design and process variation and highlight the current quality control challenges across multiple AM systems, it would be inadequate to assume a respirator protects at an equivalent level to the filter medium. Before mass sharing of the designs and subsequent fabrication and distribution of printed respirators, these potential modes of failure should be explored for their impact on filtration efficiency. Safety concerns about AM respirators have been identified [36], but their true filtration capabilities have not been measured and are not disclosed. Without this knowledge, even when properly fitted, the protection offered by an AM respirator is unknown.

1.3. Research goal

It is imperative to evaluate the performance of printed respirators to identify their ability to effectively filter nanoparticles on the size scale of the SARS-COV-2 virus. Without this knowledge, people could be using printed PPE under a false sense of security. In this work, the authors present data on high-resolution particle transmission through several respirator designs, printed in different materials and using different AM processes (i.e., desktop-scale and industrial-scale FFF systems and a PBF system). Particle removal efficiency of each respirator has been evaluated, and the results are compared to the performance of N95 respirators and cloth masks. To the authors' knowledge, this is the first quantitative data on particle transmission through respirators fabricated with AM. By thoroughly exploring the process-driven aspects leading to lower filtration efficiency, this study advances knowledge on the improvised use of AM for respirators, which will help determine whether or not the current AM processes and materials are viable options to support healthcare workers. Furthermore, the study provides better understanding of the limitations of AM in producing N95-type respiratory protection. Continued sharing of knowledge will guide design and manufacturing schemes to produce quality AM parts with high filtration efficiency.

2. Materials and methods

2.1. Respirator designs

Respirator models were selected from available, open-sourced designs based on medical professionals' recommendations and file availability. The latest designs can be found on the United States National Institutes of Health 3D Print Exchange, which provides a collection of AM PPE with monitored levels of approval for use in the COVID-19 pandemic. Standard tessellation language (STL) files of the designs listed in Table 1 were downloaded and printed without modification to the design to simulate community goals of a distributed manufacturing network to address PPE shortage during a pandemic. The abbreviations *Montana, Factoria,* and *Stopgap* will be used to distinguish each respective design. Example prints of each design are shown in Fig. 2. At the time of testing, the Montana design "…has not been fully tested [for aerosols] and has not been approved by federal or state authorities" and is not intended to replace N95 respirators [37]. The Factoria design "… has not been approved by any regulatory agency and has not passed any laboratory tests." [38] The Stopgap design "…is not suitable protection against airborne exposures and should not be used as a replacement for a N95 mask." [33] Given these statuses, it is speculated that when undergoing aerosol generation testing, none of the designs will provide 95% filtration efficiency, but with no quantifiable basis to these claims,

Table 1
Designs used for particle transmission testing and recommended parameters at the time of the study. Respirator shell thickness was estimated from the STL file.

Design Name (*Abbreviation*)	Source	Recommended Manufacturing Instructions from Source	Shell Thickness
Montana Mask V1 (*Montana*)	[37]	FFF: PLA Infill: 25 – 30%; Layer height: 0.1 to 0.2 mm	~2.4 mm
La Factoria 3D COVID-19 Mask V1 (*Factoria*)	[38]	FFF: PLA Infill: 15 – 20%; Layer height: 0.25 mm	~2.4 mm
Stopgap Surgical Face Mask Rev. A (*Stopgap*)	[33]	PBF: Nylon (blend of recycled and virgin powder) Default machine settings Post-process: de-powder, bead blast, rinse, and dry	~1.2 mm

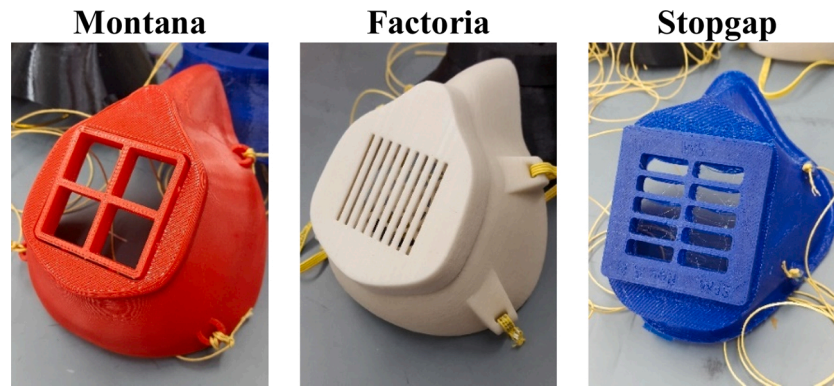## Montana   Factoria   Stopgap

Fig. 2. Example prints of each of the selected respirator designs with filter caps secured in place.

only through experiments can actual filtration efficiency be discerned as well as the reasons for such levels of performance.

The Montana and Factoria respirators are nearly identical in shape but involve different methods of securing a filter. Both of these designs feature the shell having one large, square opening in the front. The Montana respirator filter is inserted from the inside of the respirator to cover this opening, and the square cap is pushed from the inside to secure the filter. The Factoria respirator is a three-part design. The slotted front cap is removed, and the filter is placed in front of a smaller piece that locks into the shell. Then, the front cap is replaced. For the Stopgap respirator, the front cap is removed, the filter is placed over a grated design mirroring the design of the cap, and the cap is replaced.

The design files of the respirators have been updated since the study began. These newer updates focused on eliminating support material, shortening print time, or prioritizing ergonomics; the overall design remains unchanged. The specific designs used in this study are not meant to represent an exhaustive collection, but rather provide a representative sample of popular design strategies. The purpose of this study is not to evaluate specific designs but rather assess the influence of the AM process and potential failure modes of a printed respirator on particle filtration efficiency.

2.2. Materials and manufacturing

Respirators were fabricated on industrial PBF, industrial FFF, and desktop FFF systems, as indicated in Table 2, with the specific materials, machines, and relevant process parameters listed. While the original respirator designers provided some process parameters (Table 1), not all settings were disclosed. Given time constraints, effects of process parameters and post-processing conditions on respirator performance were not explored in this study. Process parameters were therefore selected based on settings previously deemed appropriate for the given material and validated through successful prior prints. There were individual

operators for each material type to best mimic a network of industrial and hobbyist operators. In this way, process parameters are less consistent than what would be desired in a rigorous experimental design. Similarly, two different spools of Afinia Premium ABS filament were used here, which would expectedly make the study more error prone compared to a controlled study of one material batch with replicates. These sources of variability must be considered since these aspects would not be controllable in a largely-distributed manufacturing scenario.

Low infill on PLA and ABS parts was intentionally selected to reflect the recommended build settings (Table 1). It would be expected that higher infill would decrease the risk of shell porosity, though print time, material consumption, and weight would increase. All respirators were fabricated with the filter cap surface oriented flush on the build plane. For post processing, some FFF models required removal of break-away supports. The PBF models were de-powdered and bead blasted to remove adhered powder and improve surface finish. Once printed, each respirator was visually inspected for defects before filtration testing.

The three respirator designs were printed once in each material/ process. Additional Stopgap respirators were printed to evaluate effects of printing orientation. Specifically, the Stopgap respirator was printed in two orientations for ABS: one with the filter cap surface flush on the build plane, and the other with the respirator rotated with the filter cap surface facing upwards and ~45° from the build plane. Both small and medium Stopgap respirators were printed in PBF nylon.

2.3. Quantitative filtration efficiency testing

Evaluation of the respirators' filtration efficiency was completed with a testing procedure adapted from the NIOSH protocol TEB-APR-STP-0059 [39]. This approach was intended to facilitate measurements of particle removal efficiency at a size of 300 nm, the size of SARS-CoV-2 particles.

Table 2
Material, machine, and process parameters selected for each AM system.

AM System	Industrial PBF	Industrial FFF	Desktop FFF	Desktop FFF
Material	Nylon-12 (Factoria: 100% recycled; Montana/Stopgap: 50% recycled / 50% virgin)	ULTEM 9085	ABS (Two different spools for two orientations)	PLA
Machine	DTM Sinterstation 2500 Plus	Stratasys Fortus 400mc	Afinia H800	Afinia H800
Nozzle Size	–	T16 tip	0.4 mm	0.4 mm
Layer Height	0.10 mm	0.25 mm	0.2 mm	0.3 mm
Laser Hatch Spacing / FFF Infill %	0.13 – 0.15 mm	100%	~15 – 20%	15%
Nozzle Temperature	–	320 °C	260 °C	210 °C
Chamber Temperature	–	95 °C	–	–
Bed Temperature	170– 174 °C	–	90 °C	50 °C
Laser Power	12 W	–	–	–

A schematic of the setup is provided in Fig. 3. The chamber was constructed from a 280 L Sigma AtmosBag supported by a customized polyvinyl chloride frame. Particles were generated from a 2% sodium chloride solution using a Collison 3-jet nebulizer (BGI MRE-3) at 22 °C and 15–20% relative humidity. A small fan was used to promote mixing inside the chamber. Clean make-up air flow to the chamber was provided through a high-efficiency particulate air filter. The size distribution of the resulting polydisperse particles had a geometric mean aerodynamic diameter of 166 nm and geometric standard deviation of 141, as measured using a scanning mobility particle sizer (TSI SMPS 3936), assuming a sodium chloride particle density of 2.165 g/cm^3.

The original intent was to secure the respirators to a full-scale manikin head with elastic, but the manikin head proved too small for the available designs, and thus created an inadequate seal between the shell and face. As such, it was determined to eliminate the shell/face interface failure mode to instead focus on the other potential sources of failure (shell porosity, filter cap/shell interface, and filter cap/filter interface). Therefore, the backs of each printed respirator were pressed into a flat slab of modeling clay, leaving only one outlet in the clay for a vacuum line, to create an approximation of a perfect shell/face seal. For all of the Stopgap respirator's first round of testing with exception of the medium nylon respirator, instead of clay, an AtmosBag and tape were used to generate this seal behind the respirator, and the vacuum line protruded from the bag.

The vacuum line connected to the particle sizer and a mass flow controller (Aalborg GFC37), both located outside of the chamber. The mass flow controller maintained flow between 14.0 and 14.5 L/min. The particle analyzer sampled at a rate of 0.3 L/min, producing a total flow rate of 14.3–14.8 L/min and a corresponding face velocity of ~10 cm/s through the respirator, assuming the breathable area through the respirator is 25 cm^2. Either N95 filtering material or ultra low particulate air (ULPA) filtering material (99% filtration efficiency) was secured according to the design requirements of each respirator. Particle concentrations and size distributions over the range of 40–1000 nm were measured through the respirators, and the results were compared to the background to calculate filtration efficiency. Each printed respirator was tested in the chamber three times; the data represents the average value with error bars representing one standard deviation.

The particle analyzer simply counts the frequency of detected nanoparticles; it does not distinguish between nanoparticles resulting from the generated aerosol and residual nanoparticles resulting from stray particulates shed from the shell. FFF processes generate aerosol emissions mainly occurring during the initial heating of the nozzle but also through the duration of the printing [40–43]. These particles, as well as loose residual powder from PBF respirators, could potentially adhere to the respirator shells and shed during testing. Addressing this concern, subsequent tests were performed with the same batch of respirators from the initial round of testing following an additional cleaning post-process. The FFF respirators were rinsed thoroughly with tap water and dried with compressed air. Since water could cause aggregation among dry powder, the cleaning step for PBF respirators involved additional compressed air followed by the application of two coats of acrylic paint to form a sealant over any remaining loose particulates. Painting additionally rids the shell of porosity. It has been shown that fine particle emission from waterborne acrylic paints is negligible after 24 h [44]. All respirators were left in a fume hood for two days following this cleaning procedure prior to testing.

To systematically explore the impact of the failure modes from Section 1.2, the Stopgap respirator was selected for further iterations of filtration testing. The Stopgap respirator had visible porosity in the printed shell (Section 3.1), and thus facilitated the evaluation of the impact of all failure modes. To evaluate the effect of the shell porosity failure mode, the entire outer surfaces (shells and caps) of the respirators made via FFF were generously coated in LORD 320/322 epoxy to eradicate pores. These respirators were left in a fume hood for four days prior to testing. To evaluate the impact of the filter cap/shell interface, tape was applied around the filter cap to reinforce its seal to the shell. The application of epoxy and paint to the respirators to address the sealing of porosity would expectedly change the tolerances between assembled parts. This would be most concerning at the filter cap/shell interface. In the design of this study, controlling the shell porosity failure mode is almost always accompanied by the sealing of the filter cap/shell interface. Thus, "epoxy coated and sealed cap" samples can be compared to solely "sealed cap" samples to isolate the failure mode effects regardless of potentially modified tolerances.

3. Results

3.1. Visual inspection of shell porosity

No observable macroscale flaws were identified in any of the printed Montana and Factoria respirators. While the PBF-printed Stopgap respirators lacked visible pores, macroscale part defects were present in all FFF builds of the Stopgap respirator, as shown in Fig. 4. Fig. 4a and b show the Stopgap respirator fabricated with ABS in two print orientations. In both parts, there are porous walls due to inter-layer defects. Changing the print orientation did not eliminate the defects, but instead shifted their location. There could be a variety of reasons for such defects in a desktop-scale FFF system (e.g., inconsistent heating, filament misfeeds, nozzle interference). Fig. 4c shows the Stopgap respirator fabricated with PLA held up to a light to enable observation of several regions of thin material along the shell. The letters, which required more complex toolpathing, were exceptionally thin. Fig. 4d displays the Stopgap respirator fabricated with ULTEM held up to a light. Macroscale pores across the entire surface that was printed flush on the build plane are observed despite this part being printed in 100% infill on an industrial-scale FFF system.

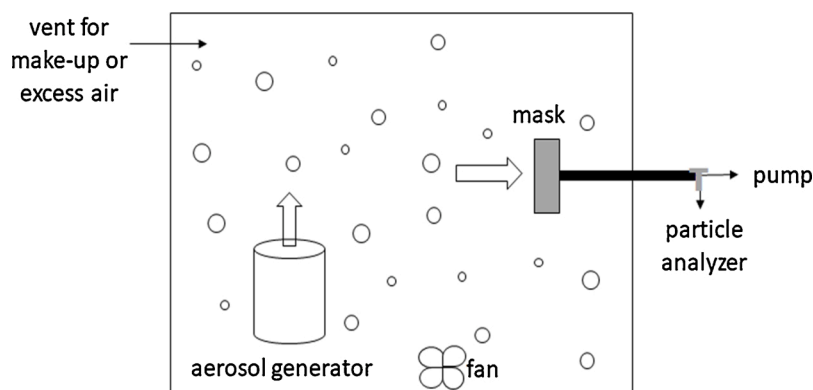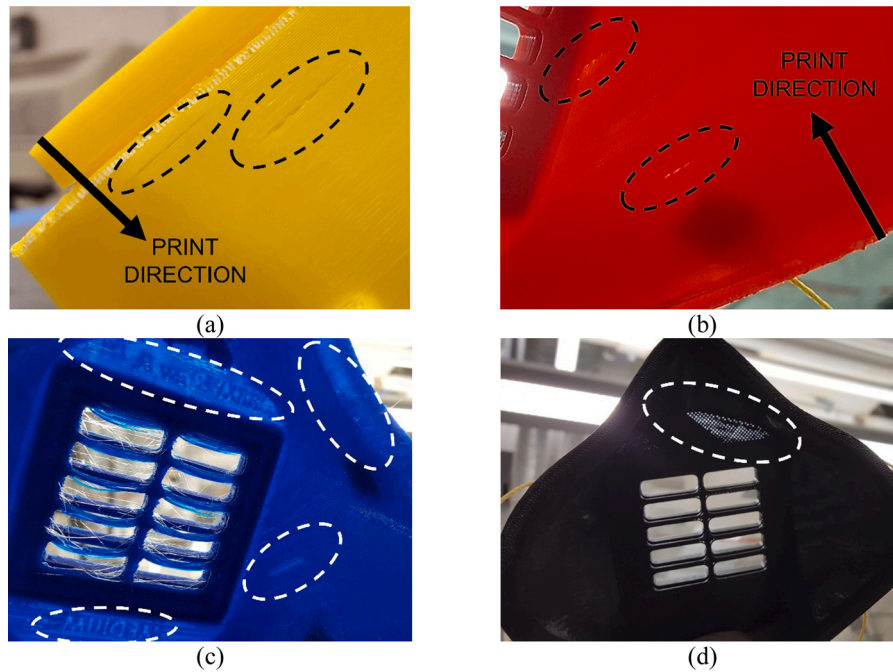It is noted that this version of the Stopgap respirator is specifically

Fig. 3. Schematic of the test setup for measuring particle transmission through the respirators.

Fig. 4. Examples of perceived defects on the respirators. (a) The Stopgap respirator in ABS oriented with the filter cap face down on the build plane has a few mislaid layers; (b) The Stopgap respirator in ABS in an alternate orientation also suffers from periodic sparsity; (c) The Stopgap respirator in PLA is visibly thin across most surfaces; (d) The Stopgap respirator in ULTEM shows porosity on the surface parallel to the filter.

designed for printing in nylon via PBF. The thin walls of the Stopgap design (Table 1), coupled with the more complex contours of the shell design relative to the other models evaluated, is likely the cause of the observable porosity in FFF prints. Although FFF-printed Stopgap respirators would not be expected to attain optimal performance, it is of interest to see how they perform relative to both the recommended PBF prints and cloth masks.

3.2. Particle transmission through the respirators

3.2.1. As-printed respirator assembly

None of the printed respirators provide protection equivalent to the inserted filter medium (either 95% or 99% filtration efficiency). Fig. 5a–c show the filtration efficiency as a function of particle diameter (i.e., Aerodynamic D_P) for the printed Montana, Factoria, and Stopgap respirators, respectively. Corresponding plots of size distribution of detected particles for this figure and those to follow are provided in Supplemental Information.

The Montana respirator results (Fig. 5a) show filtration efficiency consistently under 60% for the ABS, PLA, and nylon materials, which is far from the baseline performance of the ULPA filter medium. The ULTEM variant of the Montana respirator could not be tested as printed because the filter cap was too loose to adequately secure the filter.

The Factoria respirator results are provided in Fig. 5b. The PLA and ABS respirators filter out more particles than in the Montana respirator design, but both still only protect against ~75% of virus-sized particles. The ULTEM Factoria respirator provides the highest observed performance, with a filtration efficiency between 90–95%; however, it falls slightly less than the tested ULPA filter (99% efficiency). Similar to the Montana respirator results, the PBF-printed respirator presents the lowest filtration efficiency (~45%).

As the Montana and Factoria respirators are nearly identical in shell design, it is expected that the difference in filter cap design is the cause for the consistently worse performance of the Montana respirator compared to the Factoria respirator. The press-fit cap of the Montana respirator may have allowed particles around the filter (which correlates to the loose-fitting filter cap printed in ULTEM), whereas the larger cap

of the Factoria respirator completely encloses the filter.

All of the Stopgap samples demonstrate poor performance regardless of printing technology or material (Fig. 5c). As expected from the visible defects, the results for the FFF-printed Stopgap respirators fall the lowest of the three designs. The PBF-printed respirators, despite not having any visible defects, only offer at most ~40% filtration efficiency. As noted in Section 2.3, the particle analyzer cannot distinguish between aerosol-generated and printer-residual nanoparticles; as such, it was hypothesized that measurements were affected by the presence of residual particles on the respirators. To investigate this, the respirators were evaluated again following a cleaning procedure. Section 3.2.2 presents the results of select FFF respirators once cleaned. The results after cleaning the PBF respirators are provided with other modifications in Section 3.2.3.

3.2.2. Effect of cleaning FFF respirators

Fig. 6 shows the results of cleaned respirators, organized by material, with the initial results overlaid for comparison. It is observed in Fig. 6a that cleaning the ABS Montana respirator increases the filtration efficiency measurement by ~20%, but the ABS Factoria measurement decreases in efficiency by ~10%. The ABS Stopgap efficiency measurements significantly improve, with both print orientations offering similar performance once cleaned. In Fig. 6b, the ULTEM Factoria respirator decreases by ~15% efficiency following cleaning, and the Stopgap respirator shows marginal improvement.

These results highlight the inherent variability due to the testing method and testing conditions. The testing environment was kept as close to the same conditions when respirators were retested, yet there were inconsistent fluctuations in filtration efficiency. The lower efficiency in the Stopgap as-printed state (Fig. 5c) could be partly due to the use of the AtmosBag to seal the shell/face interface (instead of clay, as was done with all others). Tests with cloth masks have shown that even a slight gap on the shell/face interface can bring the filtration efficiency of an N95 respirator below 35% [34]. Regardless of whether the lower efficiency was caused by the seal or other factors (such as the design's more expansive surface area catching residual surface particles), the cleaned state of the FFF respirators will be used as the baseline for
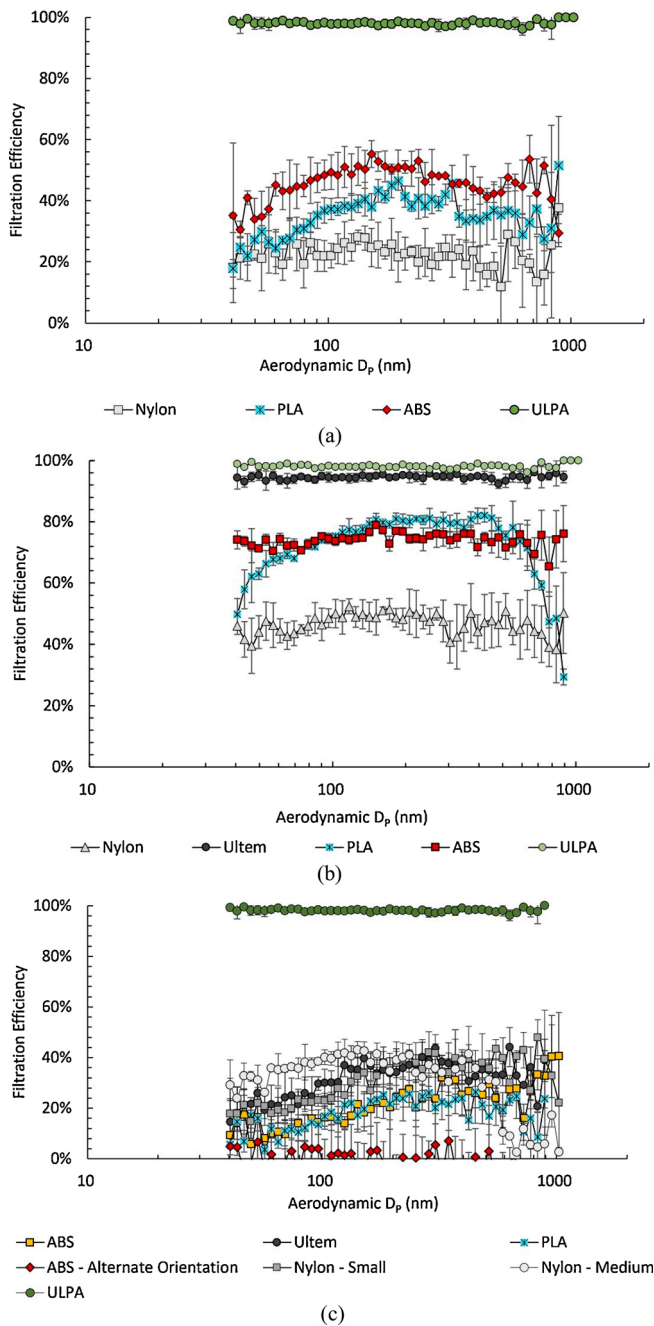
Fig. 5. Particle transmission as a function of particle diameter through respirators of various materials for the a) Montana respirator, b) Factoria respirator, and c) Stopgap respirator designs.

comparison to further tests using the Stopgap respirator.

Material shedding could not have been a significant factor for the Factoria design, which declined in filtration efficiency. It is believed that a coupling of the failure modes identified in Section 1.2 could be contributing to the erratic trends. Systematic tests were thus completed to examine the potential impacts of the individual failure modes.

3.2.3. Effect of filter cap seal and shell porosity

To assess the impact of the filter cap/shell interface and shell porosity failure modes, the filter cap seal was covered in tape and the respirators were all coated in epoxy (FFF) or paint (PBF), as described in Section 2.3. Fig. 7 presents the filtration efficiency measurements of the PLA Stopgap respirator following these separate post-processing events. It is seen that sealing the filter cap with tape does not reduce

transmission further than the baseline (cleaned) state. Application of the epoxy sealant to the shell increases efficiency to peak at ~75%. This indicates that the porosity of the PLA material drops filtration efficiency by ~20%.

The effects of post-processing the ULTEM Stopgap respirator are illustrated in Fig. 8. Although the critical failure mode for the PLA respirator is the shell porosity, the critical mode for the ULTEM respirator is the filter cap/shell interface. The application of tape at this interface improves the filtration efficiency to almost 60%, and the addition of the sealant does not yield further improvement.

Fig. 9 presents the results of modifications for the ABS Stopgap respirator. Interestingly, filtration efficiency peaks at ~65% and shows negligible improvement with the sealed cap and epoxy coat. Comparing the results from Figs. 7–9, it can be seen that with modifications, this particular respirator design shows similar peak filtration efficiency across all FFF materials. Since shell porosity, the shell/face interface, and the filter cap/shell interface have all been addressed, it is thus assumed that the fourth failure mode, the filter cap/filter interface, accounts for the lessened filtration efficiency compared to the filter medium.

Fig. 10 displays the performance of the two nylon-printed Stopgap respirators, with the as-printed state (i.e., Fig. 5c) included as the baseline. Although the respirators vary in size (small and medium), the respirators are assumed equivalent as the shell/face interface is controlled. Both respirators were cleaned with compressed air after the first round of testing, but only the size medium respirator was painted to evaluate the shell porosity failure mode. The medium respirator experiences improved filtration efficiency after being cleaned/painted, and efficiency is enhanced further when the cap is sealed. The small respirator provides similar results to the medium respirator when sealed at the cap and without painting, achieving ~90% efficiency at larger particle sizes and ~85% at smaller particle sizes. Since both fully-modified PBF respirators reach a similar peak efficiency, cleaning and sealing the filter cap/shell interface are significant, and shell porosity is not a dominant failure mode. Residual powders from printing, post-process, or handling are likely to blame for the poor performance of the respirators as-printed. This also corroborates the reason why the as-printed nylon Montana and Factoria respirators had such low filtration efficiency.

Particle transmission data for the Stopgap respirator with post-process modifications are summarized in Table 3. The values in the table are averages of all of the data points within the respective ranges.

3.3. Comparison to alternative mask materials

The respirators were compared to equivalent studies of filtration efficiency of homemade cloth masks and other materials from literature. At the advisement of the CDC, homemade fabric masks have increased in popularity and have been shown to reduce aerosol exposure to some extent. However, due to permeability, many masks made from commonplace cloth do not prevent a vast majority of droplet transmission as would a surgical mask or N95 respirator [45,46]. Fig. 11 displays filtration efficiencies of different materials across different particle size ranges from three studies compared to data from this current study at 100–300 nm. Davies and co-authors used particles that were both larger (950–1250 nm) and smaller (23 nm) than the testing range of this study [45]. Konda and co-authors used a variety of fabrics and ultimately found that layering the same fabric or mixed fabrics provided significant aerosol particle protection [34], though more layers increases the pressure drop and could impede breathability. Pan and co-authors evaluated material filtration efficiency of several commonplace cloths (evaluated over the aerosol size range of 40 to >1000 nm) as well as inward and outward protection efficiency of these materials when used as masks [47]. Fig. 11 does not accurately reflect error margins, and some materials were slightly skewed for fit; however, it does show the variability within even cloth materials as cotton could
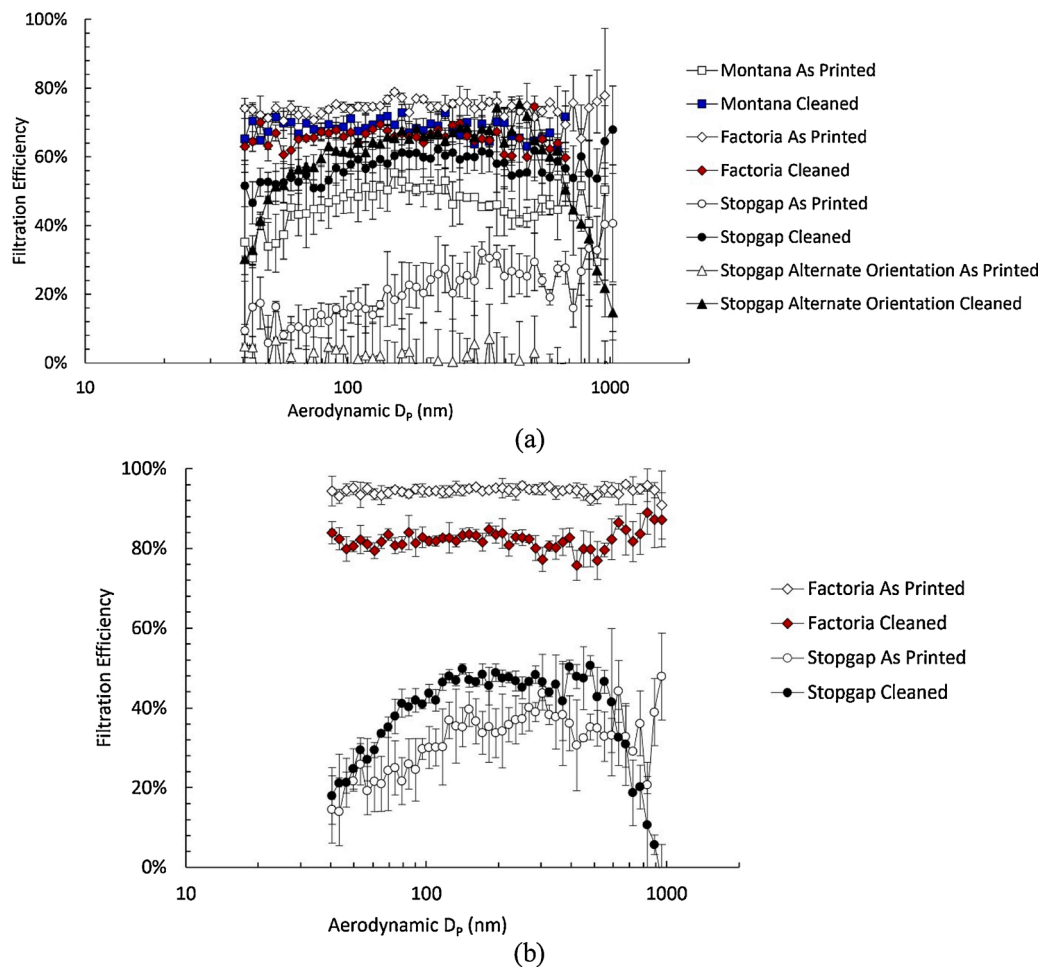
Fig. 6. Particle transmission as a function of particle diameter for various respirators in a) ABS and b) ULTEM in the as-printed state and after cleaning.
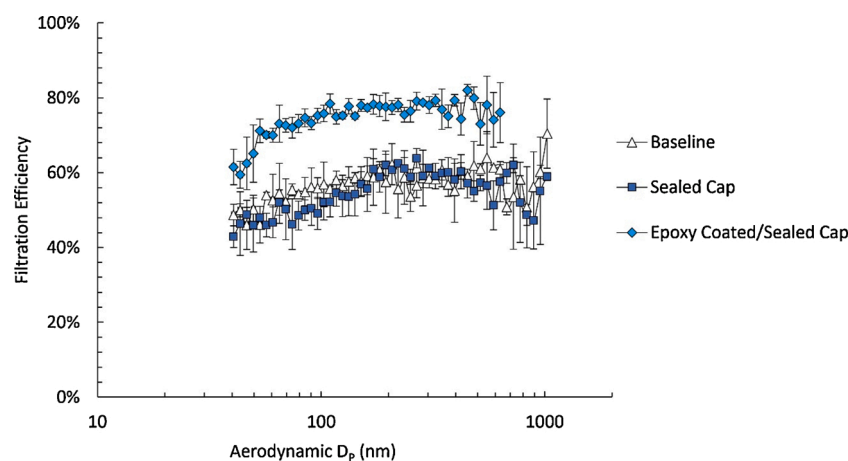

Fig. 7. Particle transmission as a function of particle diameter through the PLA Stopgap respirator.

filter 10% or >90%.

In the case of the Montana and Stopgap respirators, the as-printed performance falls below that of many simple textile materials. The as-printed Factoria respirators and post-process modified Stopgap respirators provide equivalent protection to these textile materials and surgical masks, with the ULTEM Factoria and modified PBF Stopgap respirators providing slightly enhanced performance to these materials. The modified PBF Stopgap respirators can perform better than the surgical mask, high-threaded cotton, and N95 respirator from the study by

Konda [34]. This study shows AM respirators are capable of achieving competitively high filtration efficiency on par with non-medical use masks only when assuming a perfect seal to the face. However, using AM prints strictly as face masks does not discount the need for quantitative testing and validation as they are not guaranteed to provide comparable protection to simple homemade cloth masks.
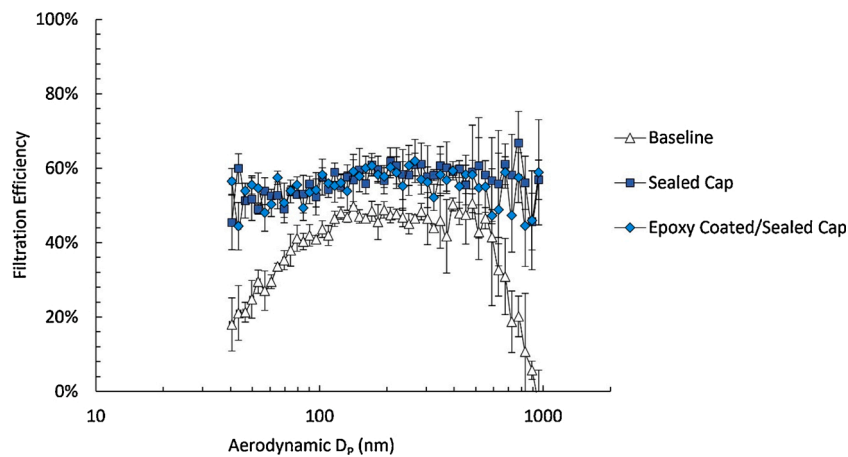
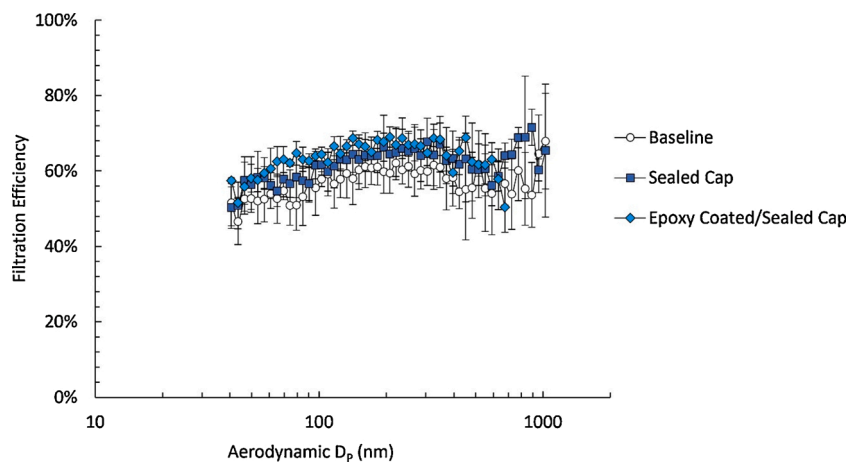**Fig. 8.** Particle transmission as a function of particle diameter through the ULTEM Stopgap respirator.

Fig. 9. Particle transmission as a function of particle diameter through the ABS Stopgap respirator.
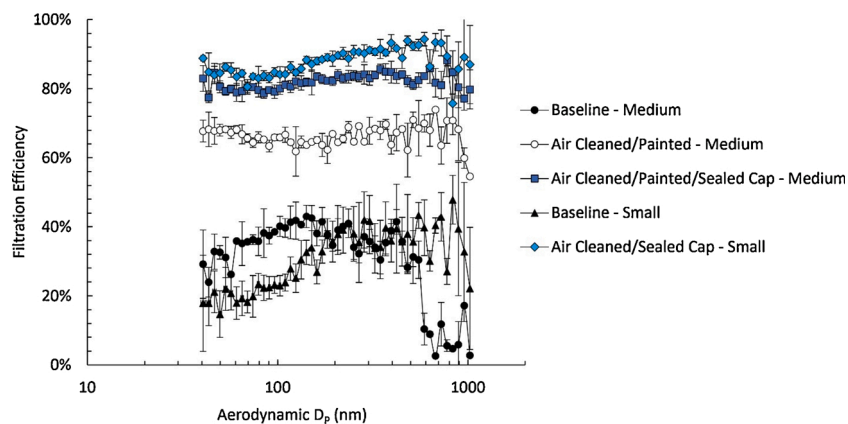
Fig. 10. Particle transmission as a function of particle diameter through the PBF (nylon) Stopgap respirator.

4. Summary and recommendations

AM enables relatively quick dissemination and production of respi-rator designs and offers potential for rapid, distributed, and democra-tized production in times of crisis. Many respirator designs have been shared to print at home and on industrial systems in response to the international PPE shortage during the COVID-19 pandemic, but little to no quantitative testing of their filtration efficiency has been made available. This study evaluated three respirator designs manufactured

with four materials on desktop and industrial FFF and PBF AM systems. The respirators were tested for particle transmission at the size of the SARS-CoV-2 virus (300 nm). Failure modes that could be appropriate for any AM respirator design were identified and sequentially evaluated to understand why AM respirators exhibited certain filtration efficiencies.

As printed, most of the respirators performed poorly, with almost all providing less than 60% filtration efficiency (significantly below the requisite 95% efficiency of an N95 respirator). This result is especially discouraging when considering that the testing was done with the

Table 3
Summary of filtration efficiency (average % ± one standard deviation) for the Stopgap Respirator with modifications at small and large particle sizes.

Material	Modification	Filtration Efficiency % (with respect to particle size)	
		40 – 300 nm	300 – 1000 nm
PLA	Baseline (Cleaned)	55 ± 4	59 ± 5
	Sealed Cap	53 ± 6	57 ± 4
	Epoxy Coated & Sealed Cap	74 ± 5	77 ± 3
ULTEM	Baseline (Cleaned)	40 ± 10	37 ± 14
	Sealed Cap	56 ± 4	58 ± 4
	Epoxy Coated & Sealed Cap	56 ± 4	54 ± 5
ABS	Baseline (Cleaned)	56 ± 4	58 ± 4
	Sealed Cap	61 ± 4	64 ± 4
	Epoxy Coated & Sealed Cap	64 ± 4	63 ± 5
Nylon – Medium	Baseline	37 ± 5	22 ± 14
	Air Cleaned & Painted	66 ± 2	67 ± 5
	Air Cleaned & Painted & Sealed Cap	81 ± 2	83 ± 3
Nylon – Small	Baseline	27 ± 8	37 ± 6
	Air Cleaned & Sealed Cap	86 ± 3	90 ± 4

approximation of a perfect seal between the respirator and user's face (a common failure mode for standard N95 textile respirators, and likely a significant failure mode for the rigid printed polymers). When printed in ULTEM on an industrial-scale FFF system, the Factoria respirator provided the best filtration efficiency of those evaluated, consistently exceeding 90% efficiency for all particle sizes.

Post-processing modifications to the printed respirators generally improved performance. Although cleaned FFF respirators did not show consistent changes in filtration efficiency measurements, cleaned PBF respirators showed higher filtration efficiencies. After modifications to sequentially account for shell porosity and the filter cap/shell interface, dominant failure modes were identified as being coupled with material and machine parameters. Because all other failure modes were accounted for via post-process treatments, and filtration efficiency of the respirators failed to reach the filter medium criteria, the filter cap/filter interface is the remaining source of leakage. Depending on respirator design, the filter may slightly shift around, allowing particles to circumvent it. This source of failure suggests future design initiatives should focus on identifying other mechanisms for securing the filter material and/or improving the interfacial tolerances.

The resource costs for additional cleaning, painting, and taping are negligible per respirator. The amount of epoxy coating used is estimated to be $5 per respirator. The biggest post process cost, however, is the required labor investment, which would challenge higher-volume production. For individual respirators, cleaning and taping were completed under five minutes, but painting and epoxy coating required more time to apply multiple coats and dry. Batch washing and dip coating paint could be administered for scaled up production, but taping and epoxy coating would likely still need to be done by hand.

The respirator design file supplements mention that the respirators should not be used as N95 equivalents, and the results from this study lend quantitative support to validate these claims and offer insight to guide future optimization efforts. Many AM drawbacks are intuitively known and thoroughly qualified, but these findings isolate application-specific failure mechanisms so that the limits of the manufacturing systems can be better understood. Failure modes such as porosity and filter seals are generalizable across multiple AM platforms. If designers are aware of these process-level constraints when fine-tuning parameters for a selected machine/material combination, it will be easier to screen emerging designs for qualitative effectiveness prior to testing.

The results from this study do not completely discount AM from being appropriate for making an effective N95 respirator. The ULTEM Factoria's performance suggests that (i) high-quality, repeatable printing technology with (ii) proper process settings, and (iii) tolerancing of the filter cap/shell interface that is aligned with a specific machine/material combination could provide an effective solution. However, different printers, materials, and process settings will not produce equivalent results, and these variables are coupled with the design of the AM respirator to affect performance. Thus, respirators fabricated by AM cannot be trusted without rigorous testing.

Those interested in developing protective AM respirators should be aware that there is more to consider than simply blindly printing or modifying a design when developing suitable respirators with high filtration efficiency. For example, without accounting for wall thickness and organic shell shape together with FFF extrusion parameters, the dangers of spurious porosity could go unseen. It is also recommended that every printed respirator manufacturer conduct similar aerosol transmission tests. Furthermore, it is essential for each user to undergo a fit test to address both anatomical fit (because it is likely that the shell/face interface causes leakage due to the rigid nature of the shell) and the user's wearing of the respirator.

The original intent of capitalizing on the opportunity to broadly, digitally distribute respirator designs to simply download, print, and immediately wear has brought about previous concerns [48], and this
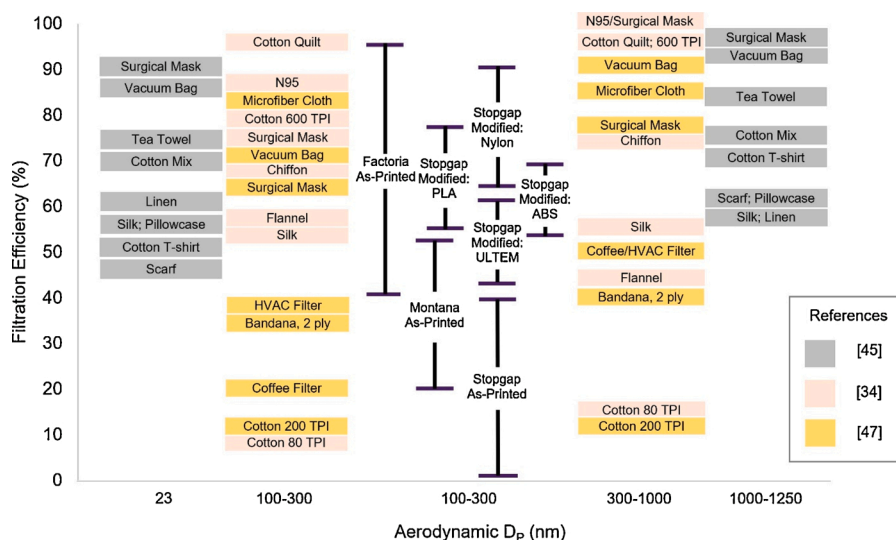
Fig. 11. Filtration efficiency of different face mask materials across different particle sizes [34,45,47] compared to data from this study. TPI, threads per inch; HVAC, heating, ventilation, and air conditioning.

study validates that a distributed respirator fabrication approach cannot yet be trusted without commensurate formal, local, quality control measures [49]. The extent to which an AM respirator protects is dependent on the material, manufacturing process, printer, and selected process parameters that complicate the ability to discern the qualitative degree of protection. A combination of identified failure modes have caused the tested respirators to perform lower than required for effective protection. Visual inspection for shell porosity is not a sufficient means for evaluating respirator performance, as the large performance deficiencies also stem from poor interfacial seals. This study has shown that interfaces are critical to adequate protection, and tolerances between printers/materials are not consistent. As the drive for innovative solutions persists, it is likely that mature respirator designs will emerge. It is imperative that thorough scientific evaluation accompany medical regulatory testing so that a rush to judgement amid anxiety does not result in unsafe practices through a false sense of security.

Declaration of Competing Interest

The authors report no declarations of interest.

Acknowledgements

Appendix A. Supplementary data

Supplementary material related to this article can be found, in the online version, at doi:https://doi.org/10.1016/j.jmsy.2021.01.002.

References

[1] Attaran M. 3D printing role in filling the critical gap in the medical supply chain during COVID-19 pandemic. Am J Ind Bus Manag 2020;10(05):988–1001. https://doi.org/10.4236/ajibm.2020.105066.

[2] N95 Respirators, Surgical Masks, and Face Masks. U.S. food & drug administration. Aug. 20. 2020. .

[3] Mandavilli A. Medical workers should use respirator masks, not surgical masks. Jun. 01. The New York Times; 2020. https://www.nytimes.com/2020/06/01/health/masks-surgical-N95-coronavirus.html.

[4] Patel P, Gohil P. Role of additive manufacturing in medical application COVID-19 scenario: India case study. Int J Ind Manuf Syst Eng 2020. https://doi.org/10.1016/j.jmsy.2020.11.006 (November).

[5] Nazir A, et al. The rise of 3D Printing entangled with smart computer aided design during COVID-19 era. Int J Ind Manuf Syst Eng 2020. https://doi.org/10.1016/j.jmsy.2020.10.009 (October).

[6] Provenzano D, et al. Rapid prototyping of reusable 3D-printed N95 equivalent respirators at the George Washington University. 2020. https://doi.org/10.20944/preprints202003.0444.v1.

[7] Tino R, et al. COVID-19 and the role of 3D printing in medicine. 3D Print Med 2020;6(1):11. https://doi.org/10.1186/s41205-020-00064-7. 7, Dec.

[8] Armani AM, Hurt DE, Hwang D, McCarthy MC, Scholtz A. Low-tech solutions for the COVID-19 supply chain crisis. Nat Rev Mater 2020. https://doi.org/10.1038/s41578-020-0205-1 (May).

[9] Swennen GRJ, Pottel L, Haers PE. Custom-made 3D-printed face masks in case of pandemic crisis situations with a lack of commercially available FFP2/3 masks. Int J Oral Maxillofac Surg 2020. https://doi.org/10.1016/j.ijom.2020.03.015. p. S0901502720301235, Apr.

[10] Sun H, Pedrielli G, Zhao G, Zhou C, Xu W, Pan R. Cyber coordinated simulation for distributed multi-stage additive manufacturing systems. Int J Ind Manuf Syst Eng 2020;57:61–71. https://doi.org/10.1016/j.jmsy.2020.07.017 (July).

[11] Neupane B, Giri B. Current understanding on the effectiveness of face masks and respirators to prevent the spread of respiratory viruses. engrXiv, preprint 2020. https://doi.org/10.31224/osf.io/h3wgc (April).

[12] Dezső G, Dezső G. Examination of layer thicknesses of a model produced by fused filament extrusion. Acta Mater Transylvanica 2019;2:13–8. https://doi.org/10.33924/amt-2019-01-03 (April 1).

[13] Ahn S, Montero M, Odell D, Roundy S, Wright PK. Anisotropic material properties of fused deposition modeling ABS. Rapid Prototyp J 2002;8:248–57. https://doi.org/10.1108/13552540210441166 (October 4).

[14] Gordeev EG, Galushko AS, Ananikov VP. Improvement of quality of 3D printed objects by elimination of microscopic structural defects in fused deposition modeling. PLoS One 2018;13:e0198370. https://doi.org/10.1371/journal.pone.0198370 (June 6).

[15] Wang X, Zhao L, Fuh JYH, Lee HP. Effect of porosity on mechanical properties of 3D printed polymers: experiments and micromechanical modeling based on X-Ray computed tomography analysis. Polymers 2019;11:1154. https://doi.org/10.3390/polym11071154 (July 7).

[16] Liao Y, et al. Effect of porosity and crystallinity on 3D printed PLA properties. Polymers 2019;11:1487. https://doi.org/10.3390/polym11091487 (September 9).

[17] Shaw B, Dirven S. Investigation of porosity and mechanical properties of nylon SLS structures. In: 2016 23rd International Conference on Mechatronics and Machine Vision in Practice (M2VIP); 2016. p. 1–6. https://doi.org/10.1109/M2VIP.2016.7827297. Nov.

[18] McCullough EJ, Yadavalli VK. Surface modification of fused deposition modeling ABS to enable rapid prototyping of biomedical microdevices. J Mater Process Technol 2013;213:947–54. https://doi.org/10.1016/j.jmatprotec.2012.12.015 (June 6).

[19] Pranzo D, Larizza P, Filippini D, Percoco G. Extrusion-based 3D printing of microfluidic devices for chemical and biomedical applications: a topical review. Micromachines 2018;9:374. https://doi.org/10.3390/mi9080374 (July 8).

[20] Ahn S, Lee CS, Jeong W. Development of translucent FDM parts by post-processing. Rapid Prototyp J 2004;10:218–24. https://doi.org/10.1108/13552540410551333 (September 4).

[21] Bae C-J, Diggs AB, Ramachandran A. Quantification and certification of additive manufacturing materials and processes. Additive manufacturing. Elsevier; 2018. p. 181–213.

[22] Es-Said OS, Foyos J, Noorani R, Mendelson M, Marloth R, Pregger BA. Effect of layer orientation on mechanical properties of rapid prototyped samples. Mater Manuf Process 2000;15:107–22. https://doi.org/10.1080/10426910008912976 (January 1).

[23] Chin Ang K, Fai Leong K, Kai Chua C, Chandrasekaran M. Investigation of the mechanical properties and porosity relationships in fused deposition modelling-fabricated porous structures. Rapid Prototyp J 2006;12:100–5. https://doi.org/10.1108/13552540610652447 (March 2).

[24] Kacmarcik J, Spahic D, Varda K, Porca E, Zaimovic-Uzunovic N. An investigation of geometrical accuracy of desktop 3D printers using CMM. IOP Conf Ser Mater Sci Eng 2018;393:012085. https://doi.org/10.1088/1757-899X/393/1/012085 (August).

[25] Lopes AJ, Perez MA, Espalin D, Wicker RB. Comparison of ranking models to evaluate desktop 3D printers in a growing market. Addit Manuf 2020:101291. https://doi.org/10.1016/j.addma.2020.101291 (May).

[26] Roberson DA, Espalin D, Wicker RB. 3D printer selection: a decision-making evaluation and ranking model. Virtual Phys Prototyp 2013;8:201–12. https://doi.org/10.1080/17452759.2013.830939 (September 3).

[27] Okwuosa TC, Soares C, Gollwitzer V, Habashy R, Timmins P, Alhnan MA. On demand manufacturing of patient-specific liquid capsules via co-ordinated 3D printing and liquid dispensing. Eur J Pharm Sci 2018;118:134–43. https://doi.org/10.1016/j.ejps.2018.03.010 (June).

[28] Khabia S, Jain KK. Comparison of mechanical properties of components 3D printed from different brand ABS filament on different FDM printers. Mater Today Proc 2020. https://doi.org/10.1016/j.matpr.2020.02.600. p. S2214785320313559, Mar.

[29] Toth-Taşcău M, Raduta A, Stoia DI, Locovei C. Influence of the energy density on the porosity of polyamide parts in SLS process. Solid State Phenom 2012;188:400–5. https://doi.org/10.4028/www.scientific.net/SSP.188.400 (May).

[30] Flodberg G, Pettersson H, Yang L. Pore analysis and mechanical performance of selective laser sintered objects. Addit Manuf 2018;24:307–15. https://doi.org/10.1016/j.addma.2018.10.001 (December).

[31] Dadbakhsh S, Verbelen L, Verkinderen O, Strobbe D, Van Puyvelde P, Kruth J-P. Effect of PA12 powder reuse on coalescence behaviour and microstructure of SLS parts. Eur Polym J 2017;92:250–62. https://doi.org/10.1016/j.eurpolymj.2017.05.014 (July).

[32] Technical considerations for additive manufactured medical devices - guidance for industry and food and drug administration staff. U.S. Food & Drug Administration; 2017. Dec. 05.

[33] Richburg C. Stopgap surgical face mask. NIH 3D Print Exchange; 2020. Apr. 03, https://3dprint.nih.gov/discover/3dpx-013429.

[34] Konda A, Prakash A, Moss GA, Schmoldt M, Grant GD, Guha S. Aerosol filtration efficiency of common fabrics used in respiratory cloth masks. ACS Nano 2020. https://doi.org/10.1021/acsnano.0c03252. p. acsnano.0c03252, Apr.

[35] Respirator trusted-source information. Centers for Disease Control and Prevention; 2020. Apr. 09, https://www.cdc.gov/niosh/npptl/topics/respirators/disp_part/respsource.html.

[36] Molitch-Hou M. Safety recommendations for 3D-printed COVID-19 medical devices, part one. Apr. 06. 3DPrint.com; 2020. https://3dprint.com/265620/safety-recomendations-for-3d-printed-covid-19-medical-devices-part-one/.

[37] The Montana Mask. Make the masks. 2021. https://www.makethemasks.com/.

[38] lafactoria3D. COVID-19 mask. Mar. 16. MakerBot Thingiverse; 2020. https://www.thingiverse.com/thing:4225667.

[39] Determination of particulate filter efficiency level for N95 series filters against solid particulates for non-powered, air-purifying respirators standard testing procedure (STP). National Institute for Occupational Safety and Health, TEB-APR-STP-0059; 2019. Dec.

[40] Vance ME, Pegues V, Van Montfrans S, Leng W, Marr LC. Aerosol emissions from fuse-deposition modeling 3D printers in a chamber and in real indoor environments. Environ Sci Technol 2017;51:9516–23. https://doi.org/10.1021/acs.est.7b01546 (September 17).

[41] Kwon O, et al. Characterization and control of nanoparticle emission during 3D printing. Environ Sci Technol 2017;51:10357–68. https://doi.org/10.1021/acs.est.7b01454 (September 18).

[42] Stephens B, Azimi P, El Orch Z, Ramos T. Ultrafine particle emissions from desktop 3D printers. Atmos Environ 2013;79:334–9. https://doi.org/10.1016/j.atmosenv.2013.06.050 (November).

[43] Deng Y, Cao S-J, Chen A, Guo Y. The impact of manufacturing parameters on submicron particle emissions from a desktop 3D printer in the perspective of emission reduction. Build Environ 2016;104:311–9. https://doi.org/10.1016/j.buildenv.2016.05.021 (August).

[44] Jørgensen RB, Hveding IG, Solheim K. Nano-sized emission from commercially available paints used for indoor surfaces during drying. Chemosphere 2017;189:153–60. https://doi.org/10.1016/j.chemosphere.2017.09.028 (December).

[45] Davies A, Thompson K-A, Giri K, Kafatos G, Walker J, Bennett A. Testing the efficacy of homemade masks: would they protect in an influenza pandemic? Disaster Med Public Health Prep 2013;7:413–8. https://doi.org/10.1017/dmp.2013.43 (August 4).

[46] van der Sande M, Teunis P, Sabel R. Professional and home-made face masks reduce exposure to respiratory infections among the general population. PLoS One 2008;3:e2618. https://doi.org/10.1371/journal.pone.0002618 (July 7).

[47] Pan J, Harb C, Leng W, Marr LC. Inward and outward effectiveness of cloth masks, a surgical mask, and a face shield. medRxiv 2020. https://doi.org/10.1101/2020.11.18.20233353. p. 2020.11.18.20233353, Jan.

[48] Clifton W, Damon A, Martin AK. Considerations and cautions for three-dimensional-printed personal protective equipment in the COVID-19 crisis. 3D Print Addit Manuf 2020. https://doi.org/10.1089/3dp.2020.0101. p. 3dp.2020.0101, Apr.

[49] 3D printing in FDA's rapid response to COVID-19. U.S. Food & Drug Administration; 2020. Aug. 03, https://www.fda.gov/emergency-preparedness-and-response/coronavirus-disease-2019-covid-19/3d-printing-fdas-rapid-response-covid-19.

[50] COVID-19 Research Projects. https://www.research.vt.edu/covid-19-updates-impacts/research.html.